Jurnal Fisika Flux: Jurnal Ilmiah Fisika FMIPA Universitas Lambung Mangkurat
Volume 20, Nomor 3, Oktober 2023
1819-796X (p-ISSN); 2541-1713 (e-ISSN)

The Effect of Shielding Material Density In Muography

Sitti Yani, Dadan Hidayatuloh, Tony Sumaryada[*)]
Department of Physics, Faculty of Mathematics and Natural Sciences, IPB University, Bogor, Indonesia

*Email korespodensi: tsumaryada@apps.ipb.ac.id

DOI: https://doi.org/10.20527/flux.v20i3.16809
Submitted: 8th July, 2023; Accepted: 31st August, 2023

ABSTRACT–In recent years, the use of high-penetrate cosmic-ray muons has been used in many applications to investigate the internal structure and composition of large material. The muon attenuation is based on multiple Coulomb scattering. This study was aimed to investigate the effect of massive shielding material composition in muography. Muon with various energies between 1 MeV to 100 MeV was used as a source located directly above the shielding material with different density and composition. The virtual detector was placed inside the shielding material and 2 km or 5 km after the shielding material.The secondary particle produced and flux of muon survived was collected in this detector. The simulation was performed using Particle and Heavy Ion Transport System (PHITS) software developed by Japan Atomic Energy Agency. The attenuation and scattering of the muon depends predominantly on the shielding material density. The muon energy and flux was decreased with increasing depth of the muon virtual detector. SiO_2 can attenuate muons better than water because SiO_2 has a greater density than water. This muography can be applied in investigating the structure and internal composition of unknown materials such as baggage inspection and volcanic structures in Indonesia.

KEYWORD : muon; muography; muon scattering, PHITS; shielding

INTRODUCTION

In recent years, muon has been used to identify the structure and composition of massive material crossed by muon, called muography, muography or muon radiography (Kaiser, 2018). This method is theoretically almost the same as X-ray imaging which is sensitive to the density of the material through which it passes. However, this method has many advantages compared to X-ray because muography applications do not require a radioactive source or artificial radiation, the source is very abundant in nature, and highly penetrating (Zhang, Enqvist, Holma, & Kuusiniemi, 2020). Muography has been applied to many kind of application and field. In the geology field, muography have been studied by (Kusagaya & Tanaka, 2015), (Tanaka, 2018), (Oláh, Tanaka, Ohminato, & Dezső, 2018), (Tioukov, et al., 2019), (Barnoud, et al., 2021). The research related with archeology using muon have been done by (Alvarez, et al., 1970), (Morishima, et al., 2017). In addition, muon was applied by (Hamar, et al., 2022) and (Cohu, et al., 2023). The ScanPyramids mission by Morishima, et al. 2017 found a big void in the Great Pyramid (Khufu's Pyramid), above the Grand Gallery using Nuclear Emulsion films from Nagoya University and Scintillator hodoscopes both inside the pyramid and reconfirmed with Gaseous chambers (CEA) outside the pyramid. Cohu et al. 2023 reconstruct 3-D image of blast furnace using muon by tracking the number of muons received by a detector, before and after passing through the furnace.

Muography can be used in baggage inspection at airports in place of the currently used x-ray as muons do no harm to the material they pass through. The materials inspected using muons are currently materials with very large volumes. This research is the

first step to find out the possibility of using muon at the airport using Monte Carlo simulation.

Muon interaction with material crossed by can be modeled using Monte Carlo (MC) simulation. MC can predict what events are experienced by particles that pass through it based on cross-sectional data and the particle's initial information provided (Nishiyama, Taketa, Miyamoto, & Kasahara, 2016). Some MC packages used in muography were PHIITS and Geant4. Particles and Heavy Ion Transport System (PHITS) was developed by Japan Atomic Energy Agency in 2006 (Niita, et al., 2006).

METHOD

All of the simulation process was done in the PHITS package (Niita, et al., 2006). The measurement technique was muography where the detector placed after the observed material. The input parameters in PHITS simulation consisted of source, material, and output. Figure 1 shows the simulation set-up where the source and detector are placed.

This study was aimed to investigate the effect of massive shielding material composition in muography. *Material*: Two materials with different density e.g. air (density = 0.00121 g/cm^3) and SiO_2 (density = 2.13 g/cm^3) were passed by the muons. The dimension of the material is 2×2×2 km^3 and 2×2×5 km^3. The energy and number of muon will be attenuated during the process.

Output (Tally): The virtual detector was placed inside the shielding material and 2 km or 5 km after the shielding material. Flux of muon survived during the simulation was recorded. The detector with dimension 100 m×100 m was recorded real-time muon crossed. Moreover, the secondary particles (photon and neutron) produced are also counted.

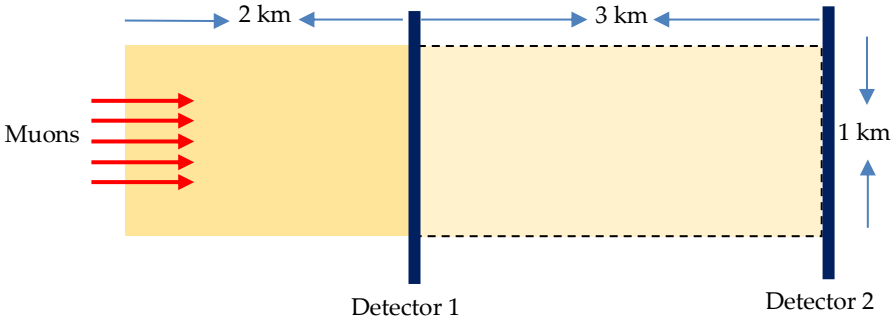

Figure 1. Simulation set-up

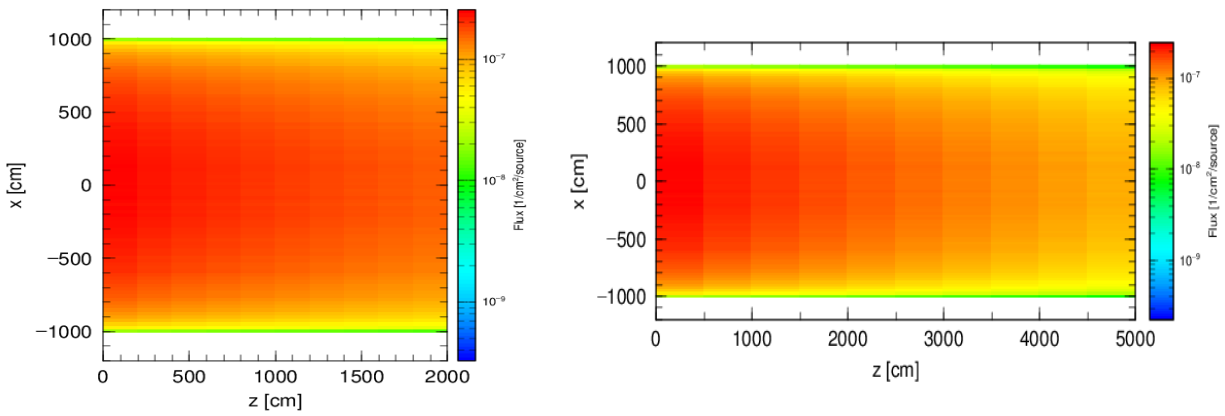

(a) 2 km (b) 5 km

Figure 2. Flux of muon in x-z plane in air material with different material thickness

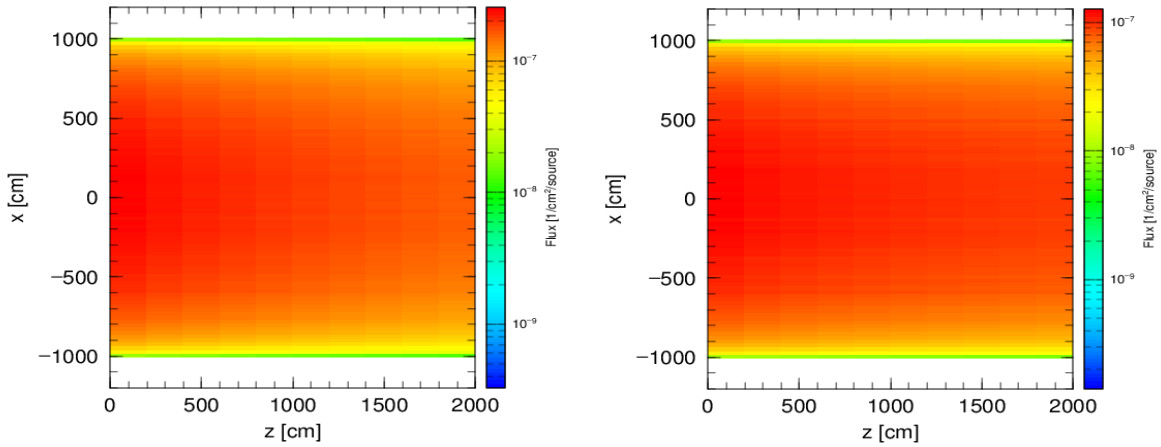

(a) 50 MeV (b) 100 MeV

Figure 3 Flux of muon in x-z plane in air material with different muon energy

RESULTS AND DISCUSSION

1. Flux of muon

Figure 2 shows the flux of muon in the x-z plane in the air material for muon energy 50 MeV. This figure shows that the amount of muon is attenuated as they interact with the material along their path. Notably, the muon flux gradually decreases with an increasing distance from the source in the z direction, evident from the color gradient transitioning from red to yellow.

Figure 3 provides a comparison of the muon fluxes at energies of 2 MeV and 5 MeV, observed at a distance of 2 km from the source. It is evident that a muon with an energy of 100 MeV travels a greater distance compared to a 50 MeV muon. As the distance increases to 500 m, there is a gradual reduction in the muon flux. Importantly, it can be observed that not all of the muon energy is attenuated at a depth of 2 km.

The variation in density between air and SiO_2 leads to a discernible disparity in the flux depicted in Figure 4. The muon flux on SiO_2 exhibits a more rapid decrease compared to the air material at the same distance and energy level. This disparity can be attributed to the higher atomic density of high-density materials, which leads to increased muon interactions and faster depletion of their energy. These results are in line with research conducted by (Lechmann, et al., 2018) studied the effect of rock composition on muon flux. Moreover, muon flux in the beam axis more than that scatter which is marked with a lighter color.

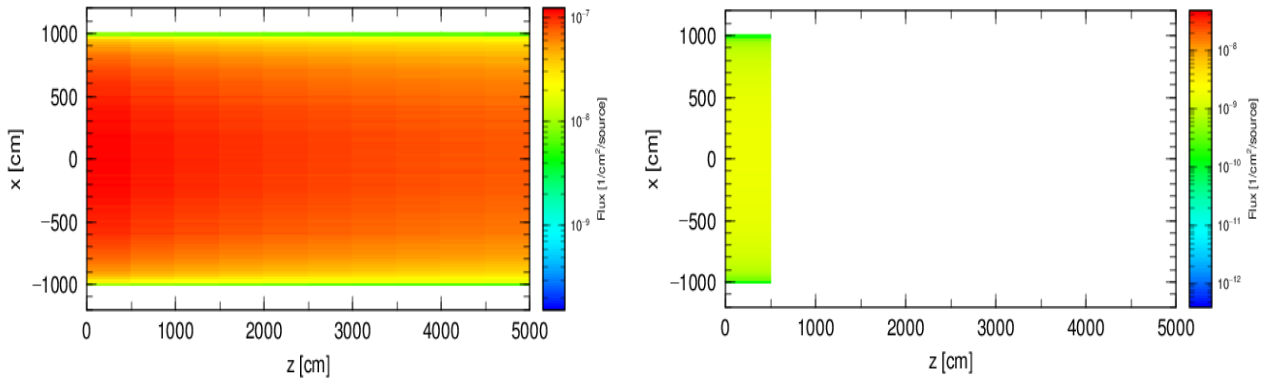

(a) Air (b) SiO_2

Figure 4 Flux of muon in x-z plane with different crossed material (energy = 50 MeV and distance 5 km)

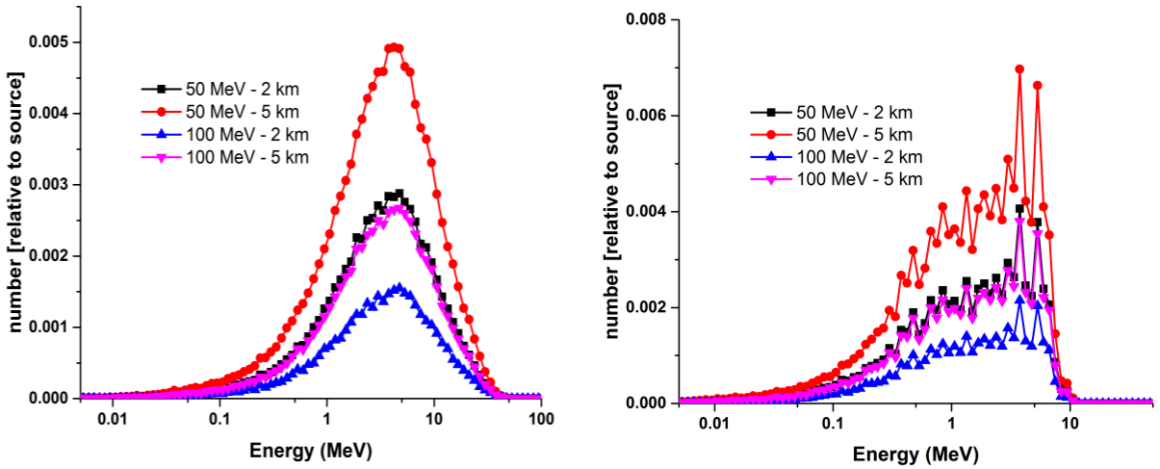

(a) Neutron (b) Photon

Figure 5 Intensity of secondary particle produced in air material with different energy and distance from source

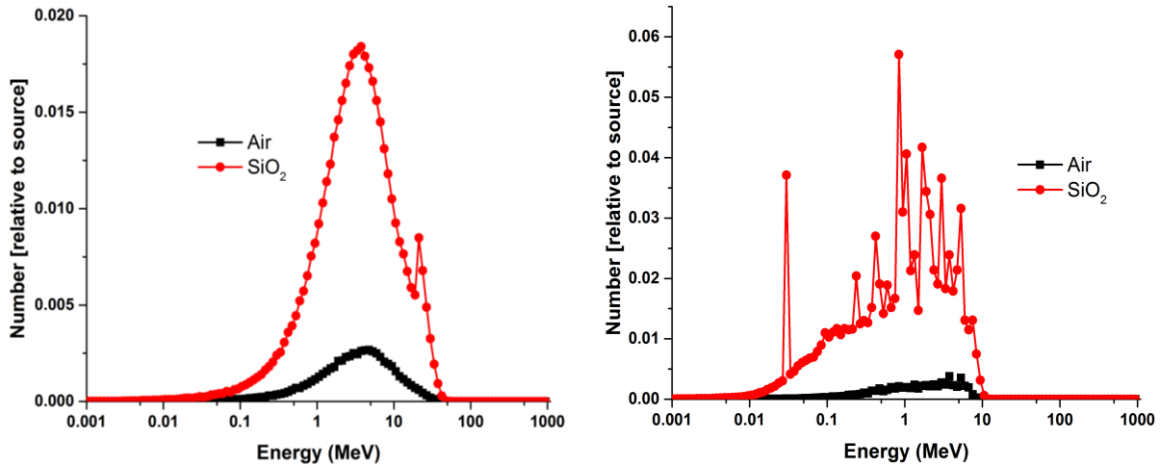

(a) Neutron (b) Photon

Figure 6 Intensity of secondary particle produced in SiO_2 and air material (muon energy: 100 MeV; material thickness: 5 km

Flux of muon in air and SiO_2 show in Figure 4. The trajectory of 100 MeV muon in SiO_2 material only reach on 500 m depth from source.

2. Secondary particles

A muon has electric charge -1 as electron when moving in a material, loses its energy almost continuously by inelastic Coulomb interaction with whole atom, electron orbitals or nuclei and is slightly scattered from its initial direction. The interaction with the atomic nuclei gives rise either to elastic/inelastic collisions or nuclear reactions and produce neutron. Moreover, the interaction with electron orbital will produce photon.

In this study, the secondary particles (photon and neutron) were analyzing for different energy and distance from source. Figure 5 show the neutron and photon produced in simulation. The average energy of neutron produced was fast neutron with energy 5 MeV. The intensity of the neutrons decreases with an increase in depth almost 2 times at a depth of 5 km for each initial muon energy. The energy of photon was bigger than neutron but the flux of this photon was less than neutron.

Figure 6 presents a comparison of the intensity of secondary particles in air and SiO_2 materials. The intensity of both neutron and photon secondary particles generated within the SiO_2 material surpasses that in the air

material. This disparity arises due to the higher atomic density inherent in high-density materials, which facilitates an increased number of interactions and subsequently leads to a higher production of secondary particles.

CONCLUSION

PHITS package can be used to simulate the interaction between muon and different material density including air and SiO_2. SiO_2 material with a density of 2.13 g/cm^3 cause muons with energies of 50 and 100 MeV cannot penetrate the material. High density materials cause an increase in the number of interactions and secondary particles produced such as photon and neutron. The energy range of neutron and photon was 0.01-50 MeV and 0.01-10 MeV, respectively. Muons can distinguish between materials with different densities, but the production of high-energy secondary particles also requires further study.

ACKNOWLEDGEMENT

This study was fully supported by Hibah Program Penelitian Dosen Muda tahun 2023 Skema Penelitian Dasar di Lingkungan Institut Pertanian Bogor (No. 11451/IT3/PT.01.03/P/B/ 2023).

REFERENCES

Alvarez, L. W., Anderson, J. A., Bedwei, F. E., Burkhard, J., Fakhry, A., Girgis, A., . . . Yazolino, L. (1970). Search for hidden chambers in the pyramids. *Science*, 832-839.

Barnoud, A., Cayol, V., Lelièvre, P. G., Portal, A., Labazuy, P., Boivin, P., & Gailler, L. (2021). Robust Bayesian Joint Inversion of Gravimetric and Muographic Data for the Density Imaging of the Puy de Dôme Volcano (France). *Front. Earth Sci.*

Cohu, A., Chevalier, A., Nechyporuk, O., Franzen, A., Sauerwald, J., Ianigro, J.-C., & Marteau, J. (2023). First 3D reconstruction of a blast furnace using muography. *Journal of Instrumentation*.

Hamar, G., Suranyi, G., Varga, D., Nyitrai, G., Olah, L., Gera, A., . . . Barnafoldi, G. G. (2022). Underground muography with portable gaseous detectors. *J. Phys.: Conf. Ser.*

Kaiser, R. (2018). Muography: overview and future directions. *Phil. Trans. R. Soc. A*.

Kusagaya, T., & Tanaka, H. K. (2015). Muographic imaging with a multi-layered telescope and its application to the study of the subsurface structure of a volcano. *Proc Jpn Acad Ser B Phys Biol Sci*, 501-10.

Lechmann, A., Mair, D., Ariga, A., Ariga, T., Ereditato, A., Nishiyama, R., . . . Vladymyrov, M. (2018). The effect of rock composition on muography measurements. *Solid Earth*, 1517–1533.

Morishima, K., Kuno, M., Nishio, A., Kitagawa, N., Manabe, Y., Moto, M., . . . Attié, D. (2017). Discovery of a big void in Khufu's Pyramid by observation of cosmic-ray muons. *Nature*, 386–390.

Niita, K., Sato, T., Iwase, H., Nose, H., Nakashima, H., & Sihver, L. (2006). PHITS—a particle and heavy ion transport code system. *Radiation Measurements*, 1080-1090.

Nishiyama, R., Taketa, A., Miyamoto, S., & Kasahara, K. (2016). Monte Carlo simulation for background study of geophysical inspection with cosmic-ray muons. *Geophysical Journal International*, 1039–1050.

Oláh, L., Tanaka, H. K., Ohminato, T., & Dezső, V. (2018). High-definition and low-noise muography of the Sakurajima volcano with gaseous tracking detectors. *Scientific Reports* .

Tanaka, H. K. (2018). Japanese volcanoes visualized with muography. *Philos Trans A Math Phys Eng Sci*.

Tioukov, V., Alexandrov, A., Bozza, C., Consiglio, L., D'Ambrosio, N., De

Lellis, G., Tanaka, H. K. (2019). First muography of Stromboli volcano . *Scientific Reports*.

Zhang, Z.-X., Enqvist, T., Holma, M., & Kuusiniemi, P. (2020). Muography and Its Potential Applications to Mining and Rock Engineering. *Rock Mechanics and Rock Engineering*, 4893–4907